



# Experimental Study on Mechanical Properties of Fully Bonded Bolts with Varied Bond Length

Houqiang Yang

Received: 12 September 2021 / Accepted: 12 April 2022 / Published online: 6 May 2022  
© The Author(s), under exclusive licence to Springer Nature Switzerland AG 2022

**Abstract** The fully bonded bolting method is widely applied in geotechnical engineering areas and is considered as an efficient approach due to its better loading capacity compared with end-anchored methods. However, the mechanical property of fully bonded bolt under various bond lengths is still unclear. This study comprises a mixed methodology of laboratorial experiments and theoretical analysis to discuss the mechanical law of fully bonded bolts under different bond lengths. Results show that the plastic debonding at the interface tends to expand as the bond length increases. Moreover, the undergoing time of the yield stage, which is between the initial and peak force stages, shows an increasing trend that is also applicable to the corresponding pull-out displacement. We have also identified that AE capturing indicated that intense energy events/values are easy to identify when the bond length increases, a phenomenon; that is closely related to the longer frictional process of the specimens with longer bond length. This study provides a reference for the design of fully bonded bolts, that is, the bond length should be carefully considered to avoid the premature failure of bolting systems due to progressive debonding.

**Keywords** Fully bonded bolt · Varied bonded length · Pull-out test · Mechanical properties

## Abbreviation

AE The acoustic emission

## 1 Introduction

Coal resources are currently the main energy sources in China (Han et al. 2015; Si et al. 2019, 2015). As an essential part of this field, fully bonded bolting method has been widely used in ground geotechnical engineering and underground coal mine engineering (Wang and Wan 2019; Wang et al. 2020; Shan et al. 2019). With the gradual mining of shallow coal resources (Zhang et al. 2019; Wang et al. 2018; Miu and Qian 2009), deep mining has become an inevitable trend of this industry (Zhang et al. 2020a, b; Zhang et al. 2020a, b; Feng et al. 2019). As illustrated in Fig. 1, under the action of deep buried high stress, the surrounding rock cracks develop and damage seriously, which decreases the bearing capacity and significantly increases the deformation sensitivity. As a result, the roadway support get more complex and prone to large deformation instability, which may lead to roof collapse accidents occurring from time to time, restricting the safe and efficient production of mine (Kang 2014). Scholars have gathered novel resources to deal with these severe issues, and proposed the concept of prestressed fully bonded bolting

---

H. Yang (✉)  
Key Laboratory of Deep Coal Resource Mining, Ministry of Education of China, School of Mines, China University of Mining and Technology, Xuzhou 221116, China  
e-mail: yhq@cumt.edu.cn



**Fig. 1** Deep buried high stress and large deformation roadway (reproduced from literature Yang et al. (2020))

method (Chen et al. 2020; Du et al. 2020; Nie et al. 2020), in which the analysis of the mechanical property is an important part (Meng et al. 2019; Zhou et al. 2017; Chen et al. 2018a, b). Even considering the complex stress of the fully bonded bolt, the bolting support design still lacks theoretical basis and deserves to be further researched (Li et al. 2019).

Research has been accruing to better understand the mechanical characteristics and supporting efficiency mechanism of the fully bonded bolt. Li et al. (2016) had conducted a series of pull-out tests of fully bonded bolts and concluded that the bond strength of the bolt was not a constant, but related to the embedment length. The bond strength was linearly proportional to the uniaxial compressive strength of the grout. Similarly, Yu et al. (2019) analyzed the critical rock bolt embedment length at which yielding or necking occurs together with the friction coefficient at the residual axial stress. They have concluded that when diameter was held constant, the maximum load and corresponding displacement increased as the cement mortar strength surged, but the residual load was still irregular.

Teymen (2017) investigated the effect of mineral admixtures on the grout strength of fully-grouted rock bolts and block punch index considering the compressive strength of the grout on the load bearing capacity. He proposed that mineral admixtures could be used for high-strength and low-cost grout in tunneling applications. Chen et al. (2017) also conducted a number of pull-out tests with a bulbed cable bolt to investigate the cylindrical specimen diameter effect on the bonding capacity and discovered that the bonding capacity increased linearly with specimen diameter up to 356 mm in the unconfined condition. In the

same year, Thenevin et al. (2017) conducted a series of laboratory pull-out tests using rock bolts and cable bolts of different materials, and confirmed the influence of confining pressure and embedment length on the pull-out response. Nie et al. (2018) analyzed the performance of the fully grouted rock bolts installed in the jointed rock mass and assumed that the reinforcement area of the reinforcement rock unit could be used to optimize their design. Moreover, they concluded that the reinforcement rock unit induced by grouped rock bolts was heavily influenced by the joint orientations and the rock bolt spacing.

Chen et al. (2018a, b) simulated the pull-out behavior of a plain cable bolt and a modified cable bolt using the commercial numerical code of FLAC2D and found that, compared with plain cable bolts, modified cable bolts could generate more confinement within the rock specimen or confinement medium. Zou and Zhang (2019) investigated the dynamic evolution characteristic of the bond strength at the interface of a bolt and a rock mass under an axial tensile load considering the non-uniform stress of the surrounding rock along the bolts. By analyzing the features of this arrangement, they have proposed a new dynamic bond-slip model.

Before these novel studies, Nemeik et al. (2014) have already presented a numerical modelling of fully grouted rock bolts loaded in tension by implementing a nonlinear bond–slip relationship of bolt–grout interface into a commercial finite difference rock mechanics code. Martin et al. (2013) also studied the bolt–grout interface of fully grouted rock bolts aiming to determine its constitutive law and proposed a semi-empirical formulation of the interface response based on the available data. A few years before this framework was proposed, Martin et al. (2011) came up with a new analytical approach that could predict the mechanical behaviour of fully grouted rock bolts subjected to pull-out tests and verified the feasibility of this method with experimental results obtained via in situ pull-out tests.

Most of the aforementioned studies focus on the laboratory pull-out test and numerical analysis calculation of the fully bonded bolt. The laboratory pull-out test mainly considers the mechanical characteristics of the fully bonded bolting system influenced by different bolt materials, bolt diameter and anchoring agent materials. Some researchers have studied the mechanical properties of the fully bonded bolt

with varied bond lengths, and achieved preliminary results. However, there is still a lack of research on the mechanical properties of fully bonded bolt specimens with different bond lengths in the yield stage under laboratorial pull-out experiment. This study aims to explore the mechanical response characteristics of fully bonded bolting specimens with different bond lengths at the yield stage, based on the condition of pull-out experiments. This study comprises a mixed methodology and laboratory experiments and theoretical analysis were carried out to reveal the mechanical law of the fully bonded bolt in the yield stage. The major outcomes presented here provide a certain reference for the design of the fully bonded supporting scheme.

## 2 Materials and Methods

### 2.1 Materials

In the first experiment, high-strength seamless steel tubes with varied lengths were used to simulate the bolt hole (Fig. 2). The inner diameter of the steel tube was 30 mm, the outer diameter was 50 mm, and the diameter of the bolt was 22 mm. Therefore, there was an 8 mm hole between the bolt rod and the inner

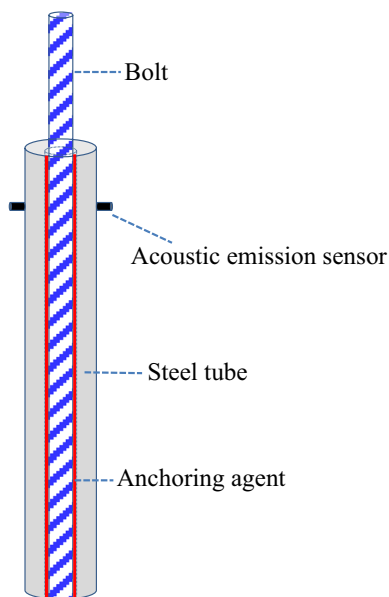


**Fig. 2** Schematic diagram of fully bonded bolts specimen

wall of the steel tube to simulate the thickness of the anchor ring. After the bolt was inserted into the steel tube, the gap between the bolt rod and the inner wall of the steel tube was filled with the anchoring agent. All the adopted bolts are all left-lateral, rib-free, and high-strength bolts, with yield strength and tensile strength of 335 MPa, 490 Mpa, respectively. The anchoring agent is a kind of prestressed duct grouting agent whose particle size is ultra-fine. The fluidity, bleeding rate, free expansion rate (24 h), initial setting time, and final setting time of the grouting agent used is 20, 1.8–2.0%, 0.18%, 5.6 h, and 16 h, respectively. After mixing with water, the anchoring agent had a high fluidity (water cement ratio was 0.32), and could easily fill the gap between the bolt and the inner wall of the steel tube. The initial setting time of the grouting agent was more than 4 h, and the final setting time was less than 24 h. The uniaxial compressive strength of the growing agent was 52.3 MPa and the uniaxial tensile strength was 2 MPa (Fig. 3).

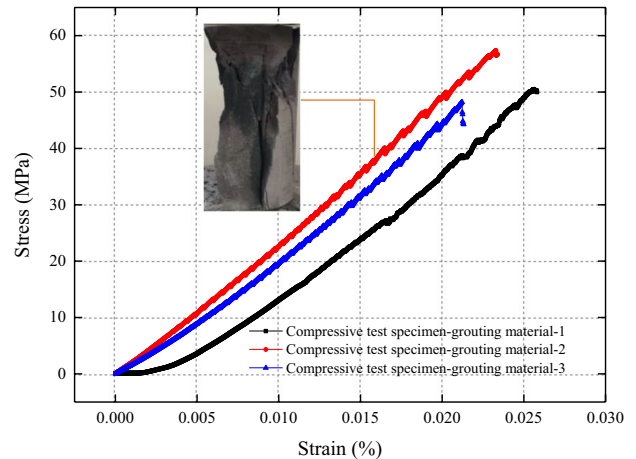
In this pull-out test of fully bonded bolt with varied bond lengths, a total of 20 left-handed, rib-free and high-strength bolts were prepared along with 20 high-strength seamless steel tubes. In addition, five groups of different schemes were set up and four identical specimens were prepared for each group to avoid the dispersion of the test. A total of 20 specimens were involved in the experiment. The steel tube length, anchor rod length and grouting agent dosage used in each group of tests are shown in Table 1. However, it is worth noting that the selection of bond length in the fully bonded bolt specimen is an essential part of this experiment. When the bond length is too large, it makes it challenging to pull out the specimen, so it breaks under pull-out conditions. In order to ensure the rationality of the experimental scheme, the bond length range of fully bonded specimens used in this study is 150–350 mm. These conditions were outlined after referring to Li et al.'s (2016) study (100–400 mm).

### 2.2 Specimen Preparation and Test Method

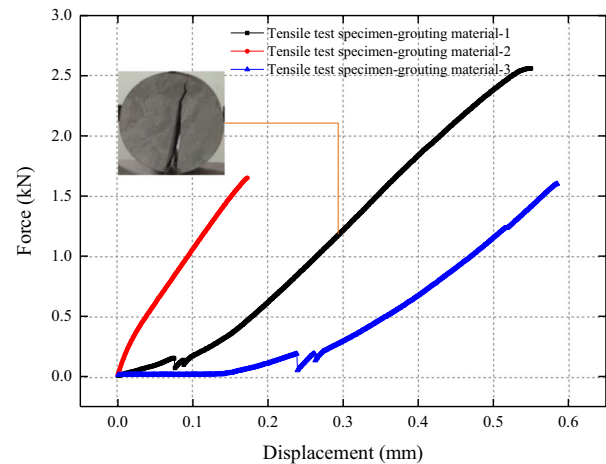
The preparation and experimental process of the specimen are as follows:

- (1) First, we inserted the bolt into the bottom of the steel tube. At this stage, the exposed length of the anchor rod is 150 mm.

**Fig. 3** Test results of specimen-grouting material strength and test specimen failure: **a** compressive test specimen-grouting material. **b** Tensile test specimen-grouting material



(a)



(b)

- (2) Then, the grouting agent with water material ratio of 0.32 was mixed evenly and poured into the gap between the bolt rod and the steel tube until the space of the whole gap is filled. At this stage, the exposed section of the bolt is 100 mm.
- (3) After the specimen preparation was completed, the grouting agent was kept at room temperature for 28 days to ensure that the final strength of grouting agent can meet the requirements of anchorage.
- (4) After 28 days of curing, the fully bonded specimens were placed on the MTS pull-out testing machine (Fig. 4). Acoustic emission technology was used to explore the internal failure mechanism of the fully bonded specimen in the failure process. Two acoustic emission probes were

installed at a distance of 50 mm from the end of the fully bonded specimen to detect the energy diffusion of crack propagation during the pull-out process. Finally, the pull-out test was carried out. The displacement control program of the MTS Criterion Model 64 during the pull-out test was 15 mm/min Feng (2017).

**Table 1** Experimental scheme and specimen preparation

ID	Length of steel tube (mm)	Length of bolt (mm)	Length of exposed section of bolt (mm)	Volume of grouting agent injected (ml)
1	200	300	150	48.99
2				
3				
4				
5	250	350	150	65.32
6				
7				
8				
9	300	400	150	81.65
10				
11				
12				
13	350	450	150	97.98
14				
15				
16				
17	400	500	150	114.31
18				
19				
20				

### 3 Results and Analyses

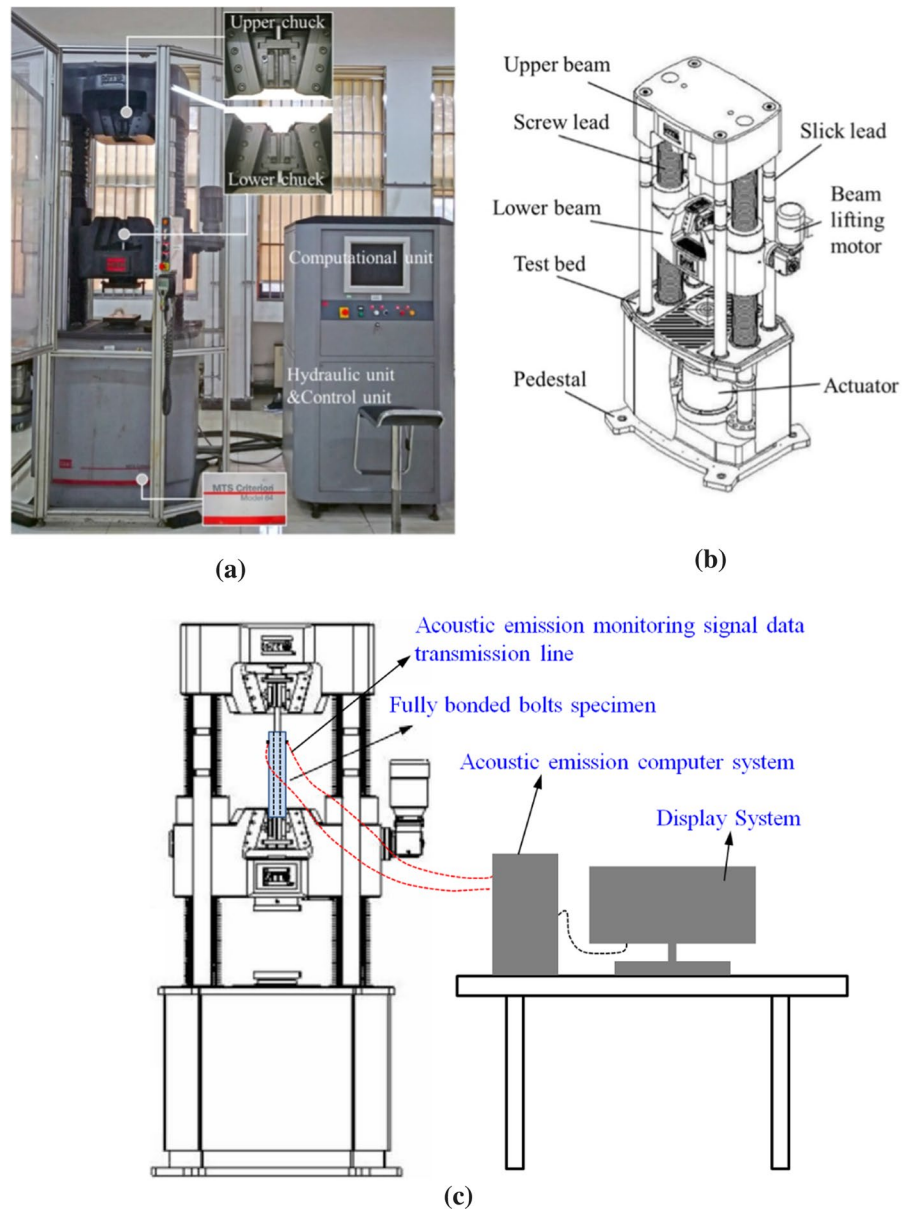
#### 3.1 Results of Mechanical Properties of Bolt During Pull-out Test

The pullout force–displacement curves of the fully bonded bolt specimen are shown in Figs. 5, 6, 7, 8, 9, with a total of 20 groups. As illustrated, all the pull-out mechanical curves of fully bonded bolt specimens show three stages. The first stage is the elastic stage in which the pull-out force increases linearly with the displacement. The second stage is the yield stage in which the slope of the curve evidently decreases before the peak pull-out force. In this stage, it is easy to detect that the displacement increases, while the drawing force is slowly surging. The third stage is the post-peak stage in which the displacement increases rapidly and the pull-out force decreases at the same speed and that is when the fully bonded bolt is pulled out. As it can be seen in Fig. 5, when the bolt length was 300 mm and the steel tube length was 200 mm, the bolt showed a trend of an approximately linear increase with the pull-out force. When the pulling displacement was 14 mm, the pull-out force reached

the peak. Afterwards, it dropped down with the increase of pulling displacement. It should be noted that specimen 1, 2, 4 did not go through the yield stage. It has been observed that their slope of the curve obviously slowed down before the bolt reached the peak pull-out force. In contrast, only specimen 3 experienced the yield stage before reaching the peak force point. It can also be concluded from the failure photos of specimen 1 that when the bolt was pulled out, the grouting agent was also pulled out without any damage. Accordingly, it could be concluded that there was almost no damage between the anchoring agent and the inner wall of the steel tube. At this time, the bolt and anchoring agent were entirely pulled out, and the pull-out force was hardly transmitted to the steel tube itself.

According to Fig. 6, when the bolt length was 350 mm, the steel tube length was 250 mm, and the displacement was 20 mm. Under these circumstances, the pull-out force reached its peak. The pull-out force–displacement curves of the four specimens all went through the tensile yield stage before reaching the peak force point. When the displacement was between 10 and 20 mm (before reaching the peak),

**Fig. 4** Rendering picture for test equipment: **a** schematic sketch of MTS Criterion 64. **b** For MTS Criterion Model 64 testing machine. **c** Experimental system diagram. (reproduced from Feng et al. (2018))



the slope of the curve slowed down and showed an upper convex type. Besides, the increase of displacement in this stage did not cause a large-scale increase on the pull-out force. According to the actual yield strength of the bolt, it could be inferred that the displacement growth in this stage was mainly caused by two features: (1) the plastic elongation of the bolt; (2) a small part of the interface debonding near the pull-out end of the bolt. The debonding here refers to the interface between the anchoring agent and the inner wall of the steel tube, which could be seen in Fig. 5.

As illustrated, the anchoring agent was pulled out without damage.

According to Fig. 7, when the bolt length was 400 mm, the steel tube length was 300 mm, and the displacement was 35 mm. Under these circumstances, the pull-out force reached the peak force point of 275 kN. Furthermore, all of the four specimens went through a more obvious tensile yield stage before reaching the peak. It should be noted that from the initial yield stage to the peak force, the displacement ranged between 10 and 35 mm,

**Fig. 5** Pull-out test results of the fully bonded bolts specimen. The length of steel tube was 200 mm, the length of bolt was 300 mm, the bond length was 200 mm, and the exposed length of bolt was 100 mm. The detected AE energy specimen was the energy evolution law of specimen 1

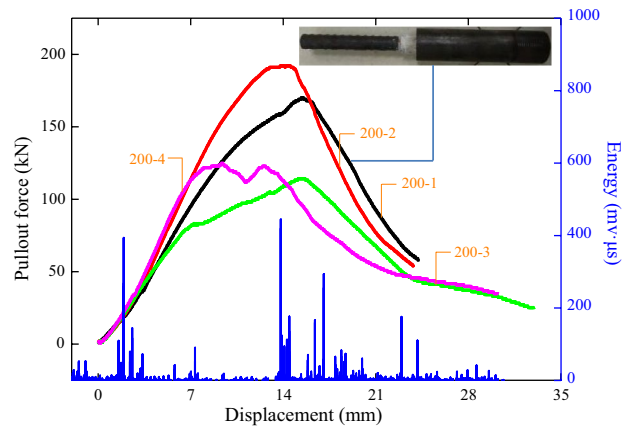


**Fig. 6** Pull-out test results of the fully bonded bolts specimen. The length of steel tube was 250 mm, the length of bolt was 350 mm, the bond length was 250 mm, and the exposed length of bolt was 100 mm. The detected AE energy specimen was the energy evolution law of specimen 2

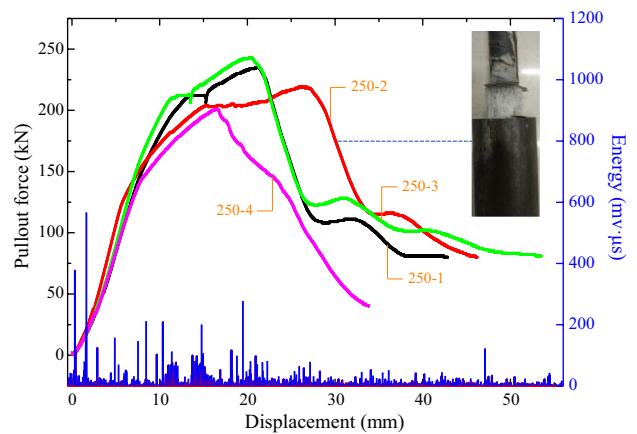
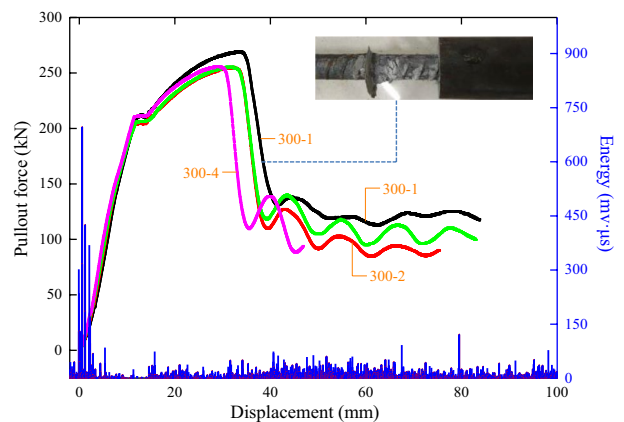


**Fig. 7** Pull-out test results of the fully bonded bolts specimen. The length of steel tube was 300 mm, the length of bolt was 400 mm, the bond length was 300 mm, and the exposed length of bolt was 100 mm. The detected AE energy specimen was the energy evolution law of specimen 1



and the four curves were quite consistent, almost without discreteness. From the failure photos of specimen 4, it can be seen that the grouting agent has been damaged, mainly due to the longer yield

stage caused by the increase of the bond length. With a longer yield stage, the grouting agent experienced stronger put-out force, which makes it more prone to be damaged.

**Fig. 8** Pull-out test results of the fully bonded bolts specimen. The length of steel tube was 350 mm, the length of bolt was 450 mm, the bond length was 350 mm, and the exposed length of bolt was 100 mm, the detected AE energy specimen was the energy evolution law of specimen 4

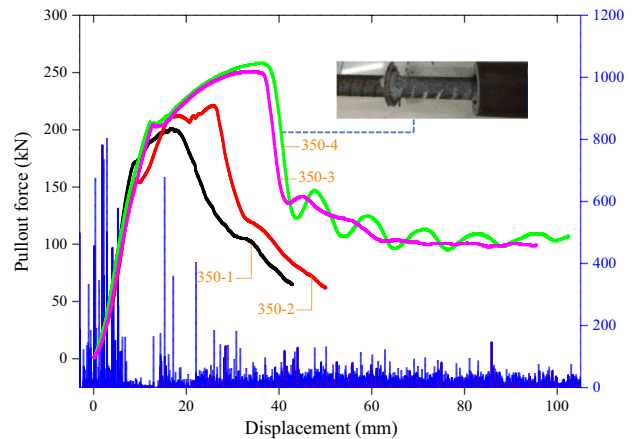
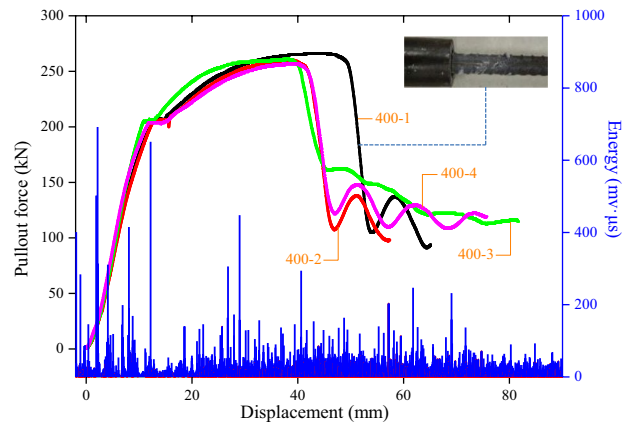


**Fig. 9** Pull-out test results of the fully bonded bolts specimen. The length of steel tube was 400 mm, the length of bolt was 500 mm, the bond length was 400 mm, and the exposed length of bolt was 100 mm. The detected AE energy specimen was the energy evolution law of specimen 1



According to Fig. 8, when the bolt length was 450 mm, the steel tube length was 350 mm, and the displacement was 39 mm. Under these circumstances, the pull-out force reached the peak force point of 280kN. Moreover, from the initial yield stage to the peak force, the displacement ranged between 10 and 35 mm. The grouting agent was also damaged after the bolt was pulled out.

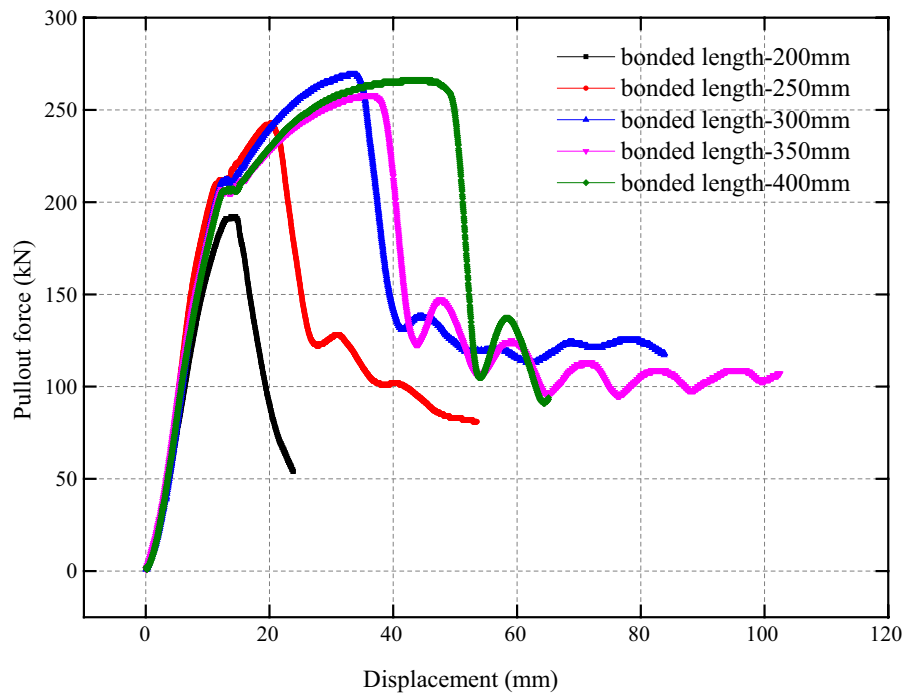
According to Fig. 9, when the bolt length was 500 mm, the steel tube length was 400 mm, and the displacement was 44 mm. Under these circumstances, the pulling force reached the peak force. Among the four specimens, the displacement corresponding to the peak force of specimen 1 reached 50 mm, which further verified that the yield stage became longer with the increase of the fully bond length.

### 3.2 Results of Acoustic Emission Energy Events During Pull-out Test

Figures 5, 6, 7, 8, 9 show that there is a positive correlation between the amount of energy in the linear growth stage of AE events and the bond length of the fully bonded bolts. This means that the longer the bond length was, the more energy events would occur at the initial stage of the bolt when bearing the pull-out force. The pull-out force also had a directly proportional correlation with the energy peak force point. Under the condition of same pull-out displacement and increased bond length, the mutual shear lag between the bond interface would undertake a stronger adjustment effect, causing the increased energy events detected by AE, and increased energy values. During the yield stage, the energy events of



**Fig. 10** Pull-out test results of the fully bonded bolts specimen with varied bond length. (Each specimen in the figure is taken from the experimental results of the specimen with smaller dispersion in each group.)



five figures were relatively small as a result of the elongation effect of the bolt when submitted to a larger pull-out force.

#### 4 Discussion

Our experiments have pointed out some interesting rules and phenomena. According to the test results of 20 groups of fully bonded bolting specimens, when their bond length ratio is small (Fig. 5), the bolts' pull-out force go through a very short yield stage before reaching the peak value. Besides, the bolt is quickly pulled out after the elastic pull-out stage rather than gradually pulled out. With the increase of the bond length (Figs. 6, 7, 8, 9), the pull-out force of the bolt goes through a longer yield stage before the peak force point. This is also the stage in which the slope of the curve before the peak pull-out force is significantly slowed down. That is, the time and the pull-out displacement increase as the bond length surges in the yield stage (Fig. 10), and the bolt is gradually pulled out under the action of the pull-out force. The reason behind this phenomenon is that when the fully bonded specimen is under the same pull-out force, the bond length of the fully bonded specimen widens,

leading to greater axial shear reaction generated at the anchorage interface in the stress yield stage, and more anchorage interface with the sudden debond of the anchorage specimen. This correlation results in a longer time of stress yield. With the increase of the fully bonded length, more energy events are likely to occur at the initial stage of the pull-out force, which also affects the energy peak. Under the condition of the same pull-out displacement of the anchor bolt, a stronger mutual shear lag adjustment effect between the bonding interface of the anchorage specimen with longer bond length, would lead to more energy events detected by acoustic emission, also increasing the energy value.

It is worth noting that after experiencing the peak pull-out force, the pull-out force value fluctuates. This is because the failure mode of the anchoring interface is progressive sliding during the pulling process of the anchor bolt. With the increase of bond length, more anchorage interfaces can be used to balance the pulling force. Due to the relationship between the force and reaction force, the pull-out force tends to be higher. The slope of the elastic growth part of the experimental curve of the fully bonded specimen remains the same, but the bond length varies because in the early stage of the

pull-out test (linear growth stage) the stressed part of the fully bonded bolting specimen is the exposed end of the bolt. So, this phenomenon is explained by the unaltered exposed length of the bolt in all fully bonded bolting specimens.

Li et al. (2016) studied the critical bond length of fully bonded bolts under different water cement ratio and found that the critical embedded length of anchor bolts is about 36 cm when the water cement ratio is 0.50 (corresponding grouting uniaxial compressive strength (UCS) is 28 MPa), a feature that is related to the embedded length. In this paper, the water cement ratio of specific ultra-fine cement used is 0.32 (UCS is 52.3 MPa). We have conducted a similar experiment and uncovered that when the bond length of the bolt exceeds 400 mm, it does not break, which may be due to the different bond ability between the grouting bond material and the steel pipe. Yu et al. (2019) studied the influence of bolt diameter on the mechanical properties of fully bonded specimens under the same cement mortar strength, but ignored the influence of anchorage bond length from the beginning to the end of the yield stage and also did not consider the progressive failure process of anchorage specimens. We consider that our results fill this literature gap since we carefully emphasized the pull-out mechanical properties of fully-bonded bolts during the whole yield stage under different conditions, e.g., same water cement ratio grouting bond material, bolt diameter, steel pipe diameter, steel pipe inner diameter, and bond lengths.

Our findings may provide guidance for the potential failure of bolt anchorage systems. Høien et al. (2021) proposed that there are three kinds of pull-out forms involved in pull-out tests: (1) pull-out below the yield strength of the bolt steel; (2) pull-out between the yield and ultimate loads, that is, during strain hardening of the steel; (3) steel failure at the ultimate load. We have identified that twenty different groups of bolts will produce corresponding yield deformation after the drawing process, which directly impacts our experimental results. Our research focused on the influence of different fully bond strengths on the mechanical properties of the anchorage system in the yield stage, but we recognized that there's still a lack of understanding regarding the influence of the bolt yield deformation on the experimental results (Fig. 10).

## 5 Conclusions

This study aimed to explore the mechanical response characteristics of the fully bonded bolts with varied bond lengths at the yield stage via a pull-out experiment. The research was carried out with a mixed methodology that comprised laboratory experiments and a theoretical analysis that could reveal the mechanical law of the fully bonded bolts in the yield stage. The major outcomes of this research led to the following conclusions:

In the pull-out test of the fully bonded bolt, the mechanical properties of varied bolt lengths in the yield stage varied greatly. When the bond length is short, the pull-out force of the bolt undergoes a short stress yield stage before reaching the peak force. In other words, the fully bonded system quickly reaches the post-peak pull-out stage after going through the elastic pull-out stage. When the bond length increases, the pull-out force of bolt undergoes a longer yield stage as a result of a larger stress anchorage interface. Both the time of yield stage and corresponding pull-out displacement get enlarged, which helps avoiding the premature pull-out of the bolt from causing fully bonded system failure. This conclusion provides a reference for the length selection of fully bonded bolts. That is, when designing the fully bonded support scheme, the length of the bolt (or the length of fully bonded bolts) should be appropriately increased in order to avoid premature debonding failure of bolt under axial tensile force.

It is noteworthy that this experiment only considers the axial pull-out of the fully bonded bolting specimen, and does not consider the lateral stress fluctuation, which is worthy of attention for future studies.

**Acknowledgements** The authors are very grateful to the reviewers for carefully reading the manuscript and providing valuable suggestions. Houqiang Yang wants to particularly thank his teachers and his girlfriend Suwan Yu for their support.

**Funding** This work was supported by the Postgraduate Research & Practice Innovation Program of Jiangsu Province (KYCX20\_2016), Future Scientists Program of China University of Mining and Technology (2020WLKXJ010).

**Data Availability** Data is contained within the article.

**Declarations**

**Conflict of interest** The authors declare no conflict interest.

## References

- Chen J, Hagan PC, Saydam S (2017) Sample diameter effect on bonding capacity of fully grouted cable bolts. *Tunn Undergr Sp Technol* 68:238–243
- Chen J, Saydam S, Hagan PC (2018a) Numerical simulation of the pull-out behaviour of fully grouted cable bolts. *Constr Build Mater* 191:1148–1158
- Chen L, Mao XB, Chen YL (2018b) Mechanical characteristics analysis of fully anchored bolts considering different post-peak failure modes of surrounding rock. *J China Coal Soc* 43:923–930
- Chen Y, Wen GP, Hu JH (2020) Analysis of deformation characteristics of fully grouted rock bolts under pull-and-shear loading. *Rock Mech Rock Eng* 53:2981–2993
- Du YL, Feng GR, Kang HP, Zhang XH, Zhang YJ, Shi XD, Wen XZ (2020) Investigation on the mechanical behavior and failure characteristics of fully grouted bolts under tension. *Energy Source A*. <https://doi.org/10.1080/15567036.2020.1829194>
- Feng XW, Zhang N, Yang S, He FZ (2018) Mechanical response of fully bonded bolts under cyclic load. *Int J Rock Mech Min Sci* 109:138–154
- Feng XW, Zhang N, Xue F, Xie ZZ (2019) Practices, experience, and lessons learned based on field observations of support failures in some Chinese coal mines. *Int J Rock Mech Min Sci*. <https://doi.org/10.1016/j.ijrmm.2019.104097>
- Han CL, Zhang N, Li BY, Si GY, Zheng XG (2015) Pressure relief and structure stability mechanism of hard roof for gob-side entry retaining. *J Cent South Univ* 22:4445–4455
- Høien AH, Li CC, Zhang N (2021) Pull-out and critical embedment length of grouted rebar rock bolts-mechanisms when approaching and reaching the ultimate load. *Rock Mech Rock Eng*. <https://doi.org/10.1007/s00603-020-02318-6>
- Kang HP (2014) Support technologies for deep and complex roadways in underground coal mines: a review. *Int J Coal Sci Technol* 1:261–277
- Li CC, Kristjansson G, Høien AH (2016) Critical embedment length and bond strength of fully encapsulated rebar rockbolts. *Tunn Undergr Sp Technol* 59:16–23
- Li YM, Zhao CX, Cong L, Meng XR, Dong CL (2019) Analysis of stress distribution characteristics of fully anchored bolt based on actual surrounding rock deformation. *J China Coal Soc* 44:2966–2973
- Martin LB, Tijani M, Hadj-Hassen F (2011) A new analytical solution to the mechanical behaviour of fully grouted rockbolts subjected to pull-out tests. *Constr Build Mater* 25:749–755
- Martin LB, Tijani M, Hadj-Hassen F, Noiret A (2013) Assessment of the bolt-grout interface behaviour of fully grouted rockbolts from laboratory experiments under axial loads. *Int J Rock Mech Min Sci* 63:50–61
- Meng XR, Zhang RF, Li YM, Jiang W, Yuan YH, Ji GQ (2019) Stress distribution law and influence factors of full-length anchorage FRP bolts. *J Min Saf Eng* 36:678–684
- Miu XX, Qian MG (2009) Research on green mining of coal resources in China: current status and future prospects. *J Min Saf Eng* 26:1–14
- Nemcik J, Ma S, Aziz N, Ren T, Geng X (2014) Numerical modelling of failure propagation in fully grouted rock bolts subjected to tensile load. *Int J Rock Mech Min Sci* 71:293–300
- Nie W, Zhao ZY, Ma SQ, Guo W (2018) Effects of joints on the reinforced rock units of fully-grouted rockbolts. *Tunn Undergr Sp Technol* 71:15–26
- Nie W, Guo W, Ma SQ, Zhao ZY (2020) Numerical modelling of fully grouted rockbolts subjected to shear load. *Rock Mech Rock Eng* 53:2493–2503
- Shan RL, Peng YH, Kong XS, Xiao YH, Yuan HH, Huang B, Zheng Y (2019) Research progress of coal roadway support technology at home and abroad. *Chin J Rock Mech Eng* 38:2377–2403
- Si GY, Shi J, Durucan S, Korre A, Lazar J, Jamnikar S, Zavsek S (2015) Monitoring and modelling of gas dynamics in multi-level longwall top coal caving of ultra-thick coal seams, Part II: numerical modelling. *Int J Coal Geol* 144:58–70
- Si GY, Durucan S, Shi J, Korre A, Cao W (2019) Parametric analysis of slotting operation induced failure zones to stimulate low permeability coal seams. *Rock Mech Rock Eng* 52:163–182
- Teymen A (2017) Effect of mineral admixture types on the grout strength of fully-grouted rockbolts. *Constr Build Mater* 145:376–382
- Thenevin I, Blanco-Martin L, Hadj-Hassen F, Schleifer J, Lubosik Z, Wrana A (2017) Laboratory pull-out tests on fully grouted rock bolts and cable bolts: results and lessons learned. *J Rock Mech Geotech Eng* 9:843–855
- Wang WJ, Wan H (2019) Mechanical characteristics analysis of fully grouted GFRP rock bolts in highly stressed soft rock tunnels. *J Min Saf Eng* 36:482–490
- Wang JH, Xie HP, Liu JZ, Wu LX, Ren SH, Jiang PF, Zhou HW (2018) Coal development and utilization theory and technical system of near-zero ecological environment impact. *J China Coal Soc* 43:1198–1209
- Wang XQ, Yang JH, Li JZ, Yang L (2020) Analysis of mechanical properties of fully-grouted bolts considering de-bonding under typical conditions. *J China Coal Soc*. <https://doi.org/10.13225/j.cnki.jccs.2020.0259>
- Yang HQ, Han CL, Zhang N, Sun YT, Pan DJ, Sun CL (2020) Long high-performance sustainable bolt technology for the deep coal roadway roof: a case study. *Sustainability-Basel* 12:1375
- Yu SS, Zhu WC, Niu LL, Zhou SC, Kang PH (2019) Experimental and numerical analysis of fully grouted long rock-bolt load transfer behavior. *Tunn Undergr Sp Technol* 85:56–66
- Zhang JX, Zhang Q, Ju F, Zhou N, Li M, Zhang WQ (2019) Practice and technique of green mining with integration of mining, dressing, backfilling and X in coal resources. *J China Coal Soc* 44:64–73
- Zhang GC, Chen LJ, Wen ZJ, Chen M, Tao GZ, Li Y, Zuo H (2020a) Squeezing failure behavior of roof-coal masses in a gob-side entry driven under unstable overlying strata. *Energy Sci Eng* 8:2443–2456
- Zhang GC, Wen ZJ, Liang SJ, Tan YL, Tian L, Zhao YQ, Zhao DS (2020b) Ground response of a gob-side entry in a longwall panel extracting 17 m-thick coal seam: a case study. *Rock Mech Rock Eng* 53:497–516

- Zhou BS, Wang BT, Liang CY, Wang YH (2017) Study on load transfer characteristics of wholly grouted bolt. *Chin J Rock Mech Eng* 36:3774–3780
- Zou JF, Zhang PH (2019) Analytical model of fully grouted bolts in pull-out tests and in situ rock masses. *Int J Rock Mech Min* 113:278–294
- Feng XW (2017) Failure mechanism and durability exploration for fully bonded bolting system. Phd Thesis Type, China University of Mining and Technology

**Publisher's Note** Springer Nature remains neutral with regard to jurisdictional claims in published maps and institutional affiliations.